# Source and thermal maturity of crude oils in the Junggar Basin in northwest China determined from the concentration and distribution of diamondoids

**Article** *in* Organic Geochemistry · January 2019

DOI: 10.1016/j.orggeochem.2019.01.004

CITATION
1

READS
198

**3 authors:**

Jiang Wenmin
Chinese Academy of Sciences
**7** PUBLICATIONS **40** CITATIONS
SEE PROFILE

Yun Li
Guangzhou Institute of Geochemistry, Chinese Academy of Science
**25** PUBLICATIONS **309** CITATIONS
SEE PROFILE

Yongqiang Xiong
Chinese Academy of Sciences
**87** PUBLICATIONS **840** CITATIONS
SEE PROFILE

Organic Geochemistry 128 (2019) 148–160

Contents lists available at ScienceDirect

Organic Geochemistry

journal homepage: www.elsevier.com/locate/orggeochem

# Source and thermal maturity of crude oils in the Junggar Basin in northwest China determined from the concentration and distribution of diamondoids

Wenmin Jiang, Yun Li *, Yongqiang Xiong

*State Key Laboratory of Organic Geochemistry (SKLOG), Guangzhou Institute of Geochemistry, Chinese Academy of Sciences, Guangzhou 510640, PR China*

ARTICLE INFO

*Article history:*
Received 29 October 2018
Received in revised form 8 January 2019
Accepted 9 January 2019
Available online 9 January 2019

*Keywords:*
Junggar Basin
Diamondoid indices
Maturity assessment
Oil–oil correlation

ABSTRACT

Here we discuss three types of diamondoid parameters for oils from the Junggar Basin. These are: absolute concentrations, concentration ratios, and isomerization ratios. According to the absolute diamondoid concentrations, the oils collected from different areas of the basin were broadly divided into three maturity stages: (1) low-mature (<100 ppm adamantanes; <5 ppm diamantanes); (2) mature (100–1000 ppm adamantanes; 5–50 ppm diamantanes); and (3) highly mature (>1000 ppm adamantanes; >50 ppm diamantanes). The oils in the northwestern region of the Junggar Basin are in the low-mature to mature stages. Based on a combination of diamondoid concentration ratios and biomarker indices, these oils can be divided into three groups, i.e., Group I oils in the Wuxia Zone derived from the lower Permian Fengcheng Formation ($P_{1f}$), Group II oils in the Kebai Zone sourced from middle Permian Lower Wuerhe Formation ($P_{2w}$), and Group III oils in the Mahu Depression generated from more mature source rocks of Jiamuhe Formation ($P_{1j}$) or the $P_{1f}$. Diamondoid concentrations and isomerization ratios were used to precisely evaluate the thermal maturity of mature oils and highly mature condensates, respectively. Our results indicate that the oils in the central part of the basin have decreasing thermal maturity from south to north, whereas the oils in the Kelameili area display increasing thermal maturity from east to west. In this study we found that different diamondoid indices are useful only in certain thermal maturity ranges. Therefore, at least for the Junggar Basin, it is crucial to know which thermal region one is in before using diamondoid ratios for maturity assessment.



## 1. Introduction

The Junggar Basin is an important oil-producing basin in northwest China (Clayton et al., 1997; Cao et al., 2005; Jin et al., 2008), located in the northern part of the Xinjiang Uygur Autonomous Region and covering an area of $1.3 \times 10^5$ km$^2$ (He et al., 2004; Li, 2005; Wei et al., 2006a) (Fig. 1a). The basin is bounded by the Kelameili and Qinggelidi mountains to the northeast, the Tianshan mountains to the south, and the Zhayier and Halalate mountains to the northwest. The tectonic units and the stratigraphic section of the Junggar Basin are shown in detail in Fig. 1a and b, respectively. The Junggar Basin is a late Palaeozoic, Mesozoic and Cenozoic superimposed basin at the junction of the Kazakhstan, Siberia, and Tarim blocks (Wang et al., 2001). It consists mainly of Carboniferous to Neogene formations that overlie basement, which consists mostly of Devonian sedimentary and metamorphic rocks (Zheng et al., 2007). It is generally considered that the basin contains six sets of source rocks (Carboniferous, Permian, Triassic, Jurassic, Cretaceous, and Paleogene) with various thermal maturities (Chen et al., 2016a, 2016b).

After several decades of exploration, more than 30 oil and gas fields have been found in the Junggar Basin. They are mainly distributed in three regions, the northwestern, central, and eastern parts of the basin (Fig. 1a). It is estimated that the oil and gas reserves in the northwestern part of the basin account for more than 40% of the total (Cao et al., 2006b). Numerous studies have demonstrated that the petroleum in the northwestern part of the basin was derived mainly from the lower Permian Jiamuhe ($P_{1j}$) and Fengcheng formations ($P_{1f}$), and the middle Permian Lower Wuerhe Formation ($P_{2w}$) of the Mahu Depression (Clayton et al., 1997; Pan et al., 2003; Cao et al., 2005, 2006b; Wang et al., 2008; Kuang et al., 2014; Chen et al., 2016a, 2016b).

* Corresponding author.
*E-mail address:* liyun@gig.ac.cn (Y. Li).

https://doi.org/10.1016/j.orggeochem.2019.01.004
0146-6380/

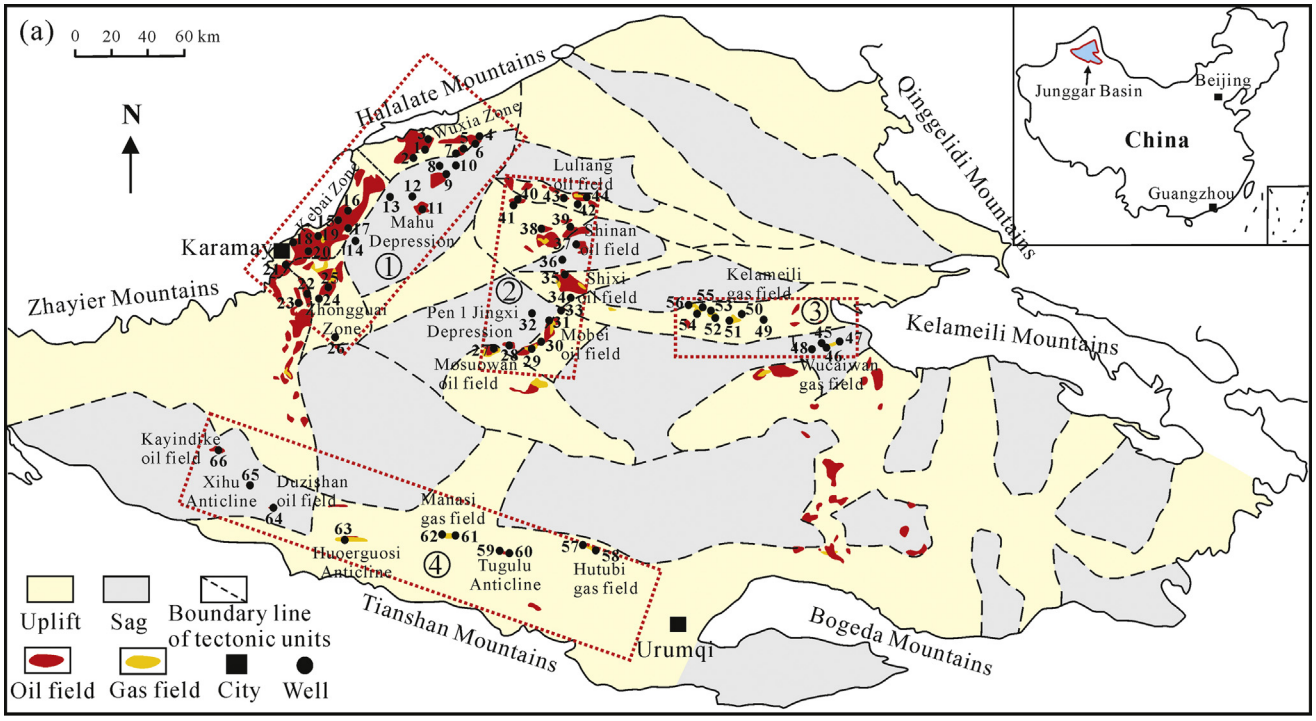


(b)

| Era | System | Series | Northwestern basin | Central basin | Southern Margin | Eastern basin |
|---|---|---|---|---|---|---|
| | | | Formation | | | |
| Cenozoic | Quaternary | Pleistocene | Xiyu ($Q_1x$) | Xiyu ($Q_1x$) | Xiyu ($Q_1x$) | Xiyu ($Q_1x$) |
| | Neogene | Pliocene | Duzishan ($N_2d$) | Duzishan ($N_2d$) | Duzishan ($N_2d$) | Duzishan ($N_2d$) |
| | | Miocene | Taxihe ($N_1t$) | Taxihe ($N_1t$) | Taxihe ($N_1t$) | Taxihe ($N_1t$) |
| | | Eocene-Oligocene | Shawan ($N_1s$) | Shawan ($N_1s$) | Shawan ($N_1s$) | Shawan ($N_1s$) |
| | Paleogene | | Wulunguhe ($E_{2-3}w$) | Anjihaihe ($E_{2-3}a$) | Anjihaihe ($E_{2-3}a$) | Anjihaihe ($E_{2-3}a$) |
| | | Paleocene-Eocene | | Ziniquanzi ($E_{1-2}z$) | Ziniquanzi ($E_{1-2}z$) | Ziniquanzi ($E_{1-2}z$) |
| Mesozoic | Cretaceous | Upper | Honglishan ($K_2h$) / Ailikehu ($K_2a$) | Donggou ($K_2d$) | Donggou ($K_2d$) | Hongshaquan ($K_2h$) |
| | | Lower | Lianmuqin ($K_1l$) | Lianmuqin ($K_1l$) | Lianmuqin ($K_1l$) | Lianmuqin ($K_1l$) |
| | | | Shengjinkou ($K_1s$) | Shengjinkou ($K_1s$) | Shengjinkou ($K_1s$) | Shengjinkou ($K_1s$) |
| | | | Hutubihe ($K_1h$) | Hutubihe ($K_1h$) | Hutubihe($K_1h$) | Hutubihe ($K_1h$) |
| | | | Qingshuihe ($K_1q$) | Qingshuihe ($K_1q$) | Qingshuihe ($K_1q$) | Qingshuihe ($K_1q$) |
| | Jurassic | Upper | | | Kalazha ($J_3k$) | Kalazha ($J_3k$) |
| | | | Qigu ($J_3q$) | | Qigu ($J_3q$) | Qigu ($J_3q$) |
| | | Middle | Toutunhe ($J_2t$) | Toutunhe ($J_2t$) | Toutunhe ($J_2t$) | Toutunhe ($J_2t$) |
| | | | Xishanyao ($J_2x$) | Xishanyao ($J_2x$) | Xishanyao ($J_2x$) | Xishanyao ($J_2x$) |
| | | Lower | Sangonghe ($J_1s$) | Sangonghe ($J_1s$) | Sangonghe ($J_1s$) | Sangonghe ($J_1s$) |
| | | | Badaowan ($J_1b$) | Badaowan ($J_1b$) | Badaowan ($J_1b$) | Badaowan ($J_1b$) |
| | Triassic | Upper | Baijiantan ($T_3b$) | Baijiantan ($T_3b$) | Haojiagou ($T_3hj$) | Haojiagou ($T_3hj$) |
| | | | | | Huangshanjie ($T_3h$) | Huangshanjie ($T_3h$) |
| | | Middle | Kelamayi ($T_2k$) | Kelamayi ($T_2k$) | Kelamayi ($T_2k$) | Kelamayi ($T_2k$) |
| | | Lower | Baikouquan ($T_1b$) | Baikouquan ($T_1b$) | Shaofanggou ($T_1s$) | Shaofanggou ($T_1s$) |
| | | | | | Jiucaiyuanzi ($T_1j$) | Jiucaiyuanzi ($T_1j$) |
| Paleozoic | Permian | Upper | Upper Wuerhe ($P_3w$) | Upper Wuerhe ($P_3w$) | Wutonggou ($P_3wt$) | Wutonggou ($P_3wt$) |
| | | | | | Quanzijie ($P_3q$) | Quanzijie ($P_3q$) |
| | | Middle | Lower Wuerhe ($P_2w$) | Lower Wuerhe ($P_2w$) | Hongyanchi ($P_2h$) | Pingdiquan ($P_2p$) |
| | | | | | Lucaogou ($P_2l$) | |
| | | | Xiazijie ($P_2x$) | Xiazijie ($P_2x$) | Jingjingzigou ($P_2jj$) | Jiangjunmiao ($P_2j$) |
| | | | | | Wulapo ($P_2wl$) | |
| | | Lower | Fengcheng ($P_1f$) | Fengcheng ($P_1f$) | Tashenkula ($P_1t$) | Jingou ($P_1jg$) |
| | | | Jiamuhe ($P_1j$) | Jiamuhe ($P_1j$) | Shirenzigou ($P_1s$) | |
| | Carboniferous | Upper | | | Aoertu ($C_2a$) | Shiqiantan ($C_2s$) |
| | | | Molaoba ($C_2m$) | | Qijiagou ($C_2q$) | |
| | | | | | Bogeda ($C_2bg$) | Bashan ($C_2b$) |
| | | Lower | Baogutu ($C_1b$) | | | Dishuiquan ($C_1d$) |
| | | | Xibeikulasi ($C_1x$) | | | |
| | | | | | | Tamugang ($C_1t$) |

**Fig. 1.** (a) Location map of the Junggar Basin showing sample locations. ①: Northwestern basin; ②: Central basin; ③: Kelameili area, Eastern basin; ④: Southern Margin of the basin and (b) the stratigraphic sequence of the Junggar Basin (after Chen et al., 2016a).

Based on more elaborate oil–source correlations using carbon isotopes and biomarkers of source rock extracts and crude oils, Chen et al. (2016a, 2016b) suggested that oils in the northwestern part of the basin originated mainly from $P_{1f}$ and $P_{2w}$ source rocks,

whereas the contribution from $P_{1j}$ source rocks was minor. Oils in the central part of the basin are considered to be generated mainly from Permian source rocks in the Pen 1 Jingxi depression (Wang, 1997; Pan et al., 1999, 2003; Yin et al., 2005; Chen et al., 2010; Wang et al., 2010). A comparison of biomarker distributions between free hydrocarbons extracted from reservoir rocks and hydrocarbons trapped in oil-bearing fluid inclusions indicate that oils produced from the central part of the basin were generated mainly from $P_{2w}$ source rocks at relatively high maturity (Pan et al., 1999).

The origins of oils in the eastern Junggar Basin are diverse and complex, with four groups of oils generated from the Carboniferous, Permian, Triassic, and Jurassic, along with mixes derived from these sources (Chen et al., 2003a, 2003b, 2004, 2016b; Wang et al., 2013). Oil and gas in the Kelameili gas field, which is the largest gas field in the Junggar Basin, are considered to be sourced from highly mature Carboniferous source rocks (Yang et al., 2002, 2012; Da et al., 2010; Long et al., 2014; Xiang et al., 2016). In addition, some oil-bearing traps have been found along the southern margin of the basin. These oils have different sources, including Permian, Jurassic, Cretaceous, and Paleogene rocks (Chen et al., 2015a, 2015b, 2016c). Due to the limited distribution of effective source rocks, only small amounts of oils are found at scattered locations along the southern margin of the basin.

Diamondoids are present in virtually all crude oils and extracts of source rocks (Williams et al., 1986; Wingert, 1992; Chen et al., 1996; Dahl et al., 1999). Due to their diamond-like structures, diamondoids are more thermally stable than most other hydrocarbons (Dahl et al., 1999), and are significantly more resistant to biodegradation (Williams et al., 1986; Wingert, 1992; Grice et al., 2000). Thus, diamondoid-based indices have been widely utilized to determine the thermal maturity of highly mature source rocks and crude oils (Chen et al., 1996; Li et al., 2000; Zhang et al., 2005), to estimate the extent of oil cracking (Dahl et al., 1999), and to evaluate biodegradation (Grice et al., 2000; Wei et al., 2007a).

The diamondoid indices that are used in this study include concentrations of adamantanes and diamantanes, concentration ratios (e.g., adamantanes/diamantanes), and isomerization ratios of diamondoids (e.g., MAI = 1-MA/(1-MA + 2-MA) and MDI = 4-MD/ (1-MD + 3-MD + 4-MD)) (The meanings of the abbreviations referred in this paper are shown in Appendix A). The construction and evaluation of diamondoid ratios are based mainly on the results of laboratory experiments (Wei et al., 2007b; Fang et al., 2012, 2013, 2015; Li et al., 2015) or on limited studies of natural samples (Chen et al., 1996; Li et al., 2000; Wei et al., 2006b). Although diamondoid ratios are considered to be potentially useful tools in multiple aspects of petroleum geochemistry, few systematic investigations have been undertaken on actual oil and gas fields. Li et al. (2018) used diamondoid ratios for source identification and maturity assessment of Tarim Basin oils; however, their study was based solely on highly mature oils. Given that the oils in the Junggar Basin were sourced from at least six sets of source rocks, with a wide range of maturity from low- to over-mature, the basin is an ideal setting for studying diamondoid indices.

## 2. Samples and methods

### 2.1. Samples

Sixty-six crude oil samples from the Junggar Basin were used in this study, comprising 12 condensates from the Kelameili gas field (eastern basin), 18 oil samples from the center of the basin, 26 oil samples from the northwestern part of the basin, and 10 oil samples from the southern margin of the basin (Fig. 1a; Table 1).

### 2.2. GC–MS analysis

Asphaltenes in the oils were removed by *n*-hexane precipitation. The de-asphaltened samples were separated into saturated and aromatic hydrocarbon fractions by silica gel and alumina column chromatography. Analyses of the saturated and aromatic fractions by gas chromatography–mass spectrometry (GC–MS) were conducted on an Agilent 7890A/5977 GC–MSD instrument equipped with an HP-5 column (30 m × 0.32 mm i.d. × 0.25 μm film thickness). The temperature of the GC oven was held at 80 °C for 2 min, then ramped to 290 °C at 4 °C/min, and finally held for 30 min at 290 °C. Helium was used as a carrier gas at a constant flow rate of 1.2 mL/min. The mass spectrometer was operated in selected ion monitoring mode for saturated fractions, monitoring *m*/*z* 85 for *n*-alkanes, *m*/*z* 191 for hopanes, and *m*/*z* 217 for steranes, and in full scan mode for aromatic fractions. The molecular ratios of aromatic or biomarker parameters were calculated by the area integration of corresponding compounds.

### 2.3. GC–MS-MS analysis

Samples for diamondoid analyses were prepared using a simple solvent dilution method. Oil samples (~50 mg) were weighed and placed in a 4 mL glass vial, which was filled with isooctane. A 100 μL internal standard (IS) solution of *n*-dodecane-$d_{26}$ and *n*-hexadecane-$d_{34}$ in isooctane was then injected into the sample vial. The standards were added after diluting the samples with isooctane, to make sure the standards were completely dissolved in the crude oils (especially the heavy oils with high viscosities); otherwise the loss of standards by evaporation may occur, affecting quantification. After 10 min of ultrasonic treatment to improve the dissolution of analytes, the vial was placed in a centrifuge for 10 min to precipitate asphaltenes and other undissolved substances. We note that researchers often use *n*-hexane to precipitate asphaltenes. In present study, as the purchased diamondoid standards we used for the calibration of diamondoid response factors were already dissolved in isooctane, the internal standards and the crude oils were also dissolved using isooctane rather than *n*-hexane.

The resulting supernatant was transferred to a 2 mL sample vial for diamondoid analysis without any further sample preparation. Gas chromatography–triple quadrupole mass spectrometry (GC–MS-MS) was conducted on the supernatant using a Thermo Fisher TSQ Quantum XLS instrument, following the method of Liang et al. (2012). Aliquots of 1 μL of each sample were injected into the GC system using an AS 3000 auto-sampler. The GC instrument was equipped with a PTV injector and a DB-1 fused silica capillary column (50 m × 0.32 mm i.d. × 0.52 μm film thickness). The PTV splitless mode was used with an inlet temperature of 300 °C, and a split flow at 15 mL/min following splitless flow for 1 min. Helium with 99.999% purity was used as a carrier gas at a constant flow rate of 1.5 mL/min. The temperature of the GC oven was held at 50 °C for 2 min, and then ramped to 80 °C at 15 °C/min, to 250 °C at 2.5 °C/min, to 300 °C at 15 °C/min, and finally held for 10 min at 300 °C. The samples were analyzed using the selected reaction monitoring (SRM) mode. The molecular ion $M^+$ was chosen as the parent ion and the corresponding base peak was used as the daughter ion except for adamantane and diamantane. In these instances, the base peak is the same as the molecular ion ($M^+$), so the most abundant fragments, *m*/*z* 93 for adamantane and *m*/*z* 131 for diamantane, were selected as the daughter ions, respectively.

The diamondoid compounds were quantified by comparing peak areas in the SRM mode between target analytes and those of the corresponding internal standards (i.e., *n*-dodecane-$d_{26}$ for adamantanes and *n*-hexadecane-$d_{34}$ for diamantanes). The

**Table 1**
Basic data for the crude oil samples from the Junggar Basin.

| Region | Zone/Oil field | Sample number | Well | Formation | Depth (m) | API gravity (°) | Viscosity (mPa s) | GOR[a] ($m^3/m^3$) | Group | Fractions (%) | | | |
|---|---|---|---|---|---|---|---|---|---|---|---|---|---|
| | | | | | | | | | | Saturates | Aromatics | Resin | Asphaltenes |
| North-western part | Wuxia zone | 1 | FN4 | $P_1f$ | 4607–4618 | 26.9 | 40.77 | 92 | I | 61.27 | 13.36 | 14.28 | 11.09 |
| | | 2 | FN7 | $P_1f_3$ | 4296–4334 | 32.1 | 15.58 | | I | 81.35 | 6.44 | 10.85 | 1.36 |
| | | 3 | W35 | $P_2w$ | 1637–1662 | 29.0 | 63.0 | | I | 66.08 | 16.37 | 15.98 | 1.57 |
| | | 4 | X71 | $P_1f$ | 4510–4530 | 31.1 | 18.64 | | I | 79.73 | 15.22 | 4.41 | 0.65 |
| | | 5 | X72 | $P_1f$ | 4808–4826 | 37.1 | 5.22 | 63 | I | 80.24 | 12.13 | 5.77 | 1.86 |
| | | 6 | X87 | | 4226–4238 | | | | I | | | | |
| | | 7 | X94 | $T_1b$ | 2914–2923 | 41.0 | 3.84 | | III | 79.69 | 9.17 | 9.95 | 1.19 |
| | Mahu depression | 8 | MA13 | $T_1b$ | 3106–3129 | 44.8 | 2.42 | 1787 | III | 81.05 | 7.76 | 10.10 | 1.09 |
| | | 9 | MA134 | $T_1b_2$ | 3169–3188 | 42.0 | 3.32 | 645 | III | 85.26 | 8.01 | 5.77 | 0.96 |
| | | 10 | MA15 | $T_1b_2$ | 3048–3056 | 47.5 | 1.59 | 1435 | III | 87.92 | 6.38 | 3.70 | 2.01 |
| | | 11 | MA18 | $T_1b$ | 3892–3920 | 40.7 | 3.94 | 171 | III | 85.08 | 9.85 | 3.88 | 1.19 |
| | | 12 | MX1 | $T_1b$ | 3582–3588 | 39.3 | 4.96 | | III | 85.17 | 8.05 | 4.23 | 2.55 |
| | | 13 | AH2 | $T_1b_2$ | 3310–3336 | 37.1 | 7.12 | | II | 80.47 | 13.28 | 5.08 | 1.17 |
| | | 14 | MH1 | $T_1b$ | 3286–3316 | 33.9 | 15.11 | 54 | II | 77.75 | 5.63 | 13.80 | 2.82 |
| | Kebai zone | 15 | B007 | C | 846–872.5 | 29.6 | 39.3 | | II | 73.52 | 12.16 | 12.52 | 1.80 |
| | | 16 | B7 | C | 1427–1437 | 32.4 | 15.8 | | II | 80.31 | 10.61 | 7.51 | 1.57 |
| | | 17 | K901 | C | 1152–1172 | 35.4 | 7.71 | | II | 81.74 | 10.53 | 7.45 | 0.28 |
| | | 18 | K92 | C | 576–588 | 32.2 | 20.36 | 110 | II | 80.03 | 9.60 | 8.93 | 1.44 |
| | | 19 | K94 | C | 1324–1350 | 36.8 | 8.93 | | II | 82.36 | 8.89 | 6.32 | 2.43 |
| | | 20 | HW5 | $T_2k$ | 648–658 | 25.3 | 105.19 | | II | 76.39 | 15.81 | 7.42 | 0.37 |
| | | 21 | HW8 | $T_2k$ | 392–395 | 28.7 | 31.67 | | II | 72.28 | 13.08 | 13.78 | 0.87 |
| | Zhongguai zone | 22 | HS4 | $T_2k$ | 1873–1876.5 | 33.2 | 16.88 | 328 | II | 83.10 | 6.81 | 6.31 | 3.78 |
| | | 23 | HS6 | C | 1046–1086 | 34.6 | 10.95 | | II | 86.92 | 6.75 | 4.62 | 1.72 |
| | | 24 | G26 | $T_2k_1$ | 2652–2655 | 38.8 | 5.72 | | III | 79.62 | 5.34 | 13.92 | 1.12 |
| | | 25 | K79 | $P_2w$ | 3521–3532 | 36.1 | 7.51 | 1143 | III | 86.33 | 5.68 | 6.77 | 1.22 |
| | | 26 | ZJ2-H | $P_1j$ | 4840.7–5760.3 | 36.1 | 11.2 | 1059 | III | 90.87 | 3.99 | 3.99 | 1.15 |
| Central part | Mosuowan oil field | 27 | P5 | $J_1s$ | 4243–4257 | 56.6 | 0.69 | 3019 | | | | | |
| | | 28 | M171 | $J_1s$ | 4318.57–4627 | 52.9 | 0.81 | 4769 | | 81.92 | 8.32 | 8.04 | 1.72 |
| | | 29 | M7 | $J_1s$ | 4239.5–4262 | 52.5 | 0.9 | 5686 | | 90.74 | 5.90 | 3.16 | 0.20 |
| | | 30 | M11 | $J_1s$ | 4136–4155 | 47.9 | 1.16 | 5320 | | 96.34 | 2.00 | 1.00 | 0.65 |
| | Mobei oil field | 31 | M001 | $J_1s$ | 3899–3910 | 48.3 | 1.23 | | | | | | |
| | | 32 | QS1 | $J_1s$ | 3943–3946.5 | 52.4 | 0.85 | 8256 | | 96.58 | 1.71 | 0.85 | 0.85 |
| | | 33 | MB11 | $J_1s$ | 3707.5–3714 | 38.6 | 6.63 | 136 | | 81.05 | 7.76 | 10.10 | 1.09 |
| | Shixi oil field | 34 | SX8 | $J_1s$ | 3382–3385 | 33.6 | 10.84 | | | 80.89 | 10.62 | 6.75 | 1.74 |
| | | 35 | SX3 | $J_2x$ | 2994–3017 | 43.1 | 1.51 | 3961 | | 85.42 | 10.41 | 4.16 | 0 |
| | Shinan oil field | 36 | SN42 | $K_1s$ | 1536–1538 | 35.7 | 5.31 | | | 84.82 | 12.40 | 2.43 | 0.35 |
| | | 37 | S303 | $K_1q$ | 2645–2655 | 39.3 | 4.73 | 41 | | 87.52 | 7.95 | 3.47 | 1.07 |
| | | 38 | S102 | $J_2t$ | 2569–2573.5 | 34.2 | 9.74 | 46 | | 76.64 | 11.48 | 9.43 | 2.45 |
| | | 39 | S123 | $J_2t$ | 2421–2428 | 33.6 | 11.09 | 171 | | 80.58 | 12.27 | 5.42 | 1.73 |
| | | 40 | XY19 | $J_1s$ | 2696–2702 | 32.4 | 14.76 | | | 83.39 | 9.20 | 6.53 | 0.89 |
| | | 41 | XY22 | $J_1s$ | 2720–2728 | 32.6 | 13.61 | | | 75.77 | 14.42 | 7.67 | 2.15 |
| | Luliang oil field | 42 | SN62 | $J_2x_4$ | 2148–2150.5 | 33.6 | 13.34 | | | 83.71 | 9.95 | 5.80 | 0.55 |
| | | 43 | L11 | $J_2t$ | 2072.5–2077 | 36.2 | 8.2 | | | 78.09 | 12.77 | 8.20 | 0.94 |
| | | 44 | L27 | $J_2x$ | 2138–2140.5 | 35.7 | 9.85 | | | 78.23 | 11.14 | 8.77 | 1.86 |
| Eastern part | Wucaiwan gas field | 45 | C25 | $C_2b$ | 3028–3038 | 57.5 | | | | | | | |
| | | 46 | C27 | $C_2b$ | 2778–2790 | 51.9 | | | | | | | |
| | | 47 | C54 | $C_2b$ | 2984–3060 | 51.5 | 0.88 | 56,956 | | 87.21 | 5.77 | 5.48 | 1.53 |
| | | 48 | C55 | C | 3348–3358 | 53.7 | 0.85 | 5422 | | 92.30 | 3.21 | 1.77 | 2.71 |
| | Kelameili gas field | 49 | DX21 | C | 2865–2876 | 46.4 | 2.0 | 33,548 | | 86.45 | 6.99 | 5.17 | 1.39 |
| | | 50 | DX33 | $C_2b$ | 3518–3526 | 57.3 | | | | | | | |
| | | 51 | D103 | C | 3050–3062 | 53.2 | 0.83 | 29,387 | | 92.91 | 3.13 | 1.71 | 2.25 |
| | | 52 | DX18 | C | 3510–3530 | 54.6 | 0.81 | 7059 | | 89.87 | 5.64 | 1.27 | 3.23 |
| | | 53 | DX27 | $J_1b$ | 2944–2949 | 55.9 | 0.63 | 95,595 | | 91.12 | 2.91 | 3.42 | 2.56 |
| | | 54 | DX14 | $P_3w$ | 3523–3550 | 50.4 | 1.02 | 14,905 | | 96.14 | 2.38 | 0.65 | 0.83 |
| | | 55 | D403 | C | 3824–3840 | 49.0 | 1.18 | 38,784 | | 96.77 | 2.14 | 0.64 | 0.45 |
| | | 56 | DX17 | C | 3662–3670 | 51.2 | 1.18 | 10,044 | | 97.52 | 0.21 | 1.97 | 0.30 |
| Southern margin | Hutubi gas field | 57 | H2 | $E_{1-2}z$ | 3594–3614 | 51.6 | | | | | | | |
| | | 58 | H2004 | $E_{1-2}z$ | 3550–3580 | | | | | | | | |
| | Tugulu anticline | 59 | TG1 | $E_{2-3}a$ | 1840–1855 | | | | | | | | |
| | | 60 | TG2 | $E_{2-3}a$ | 1507.5–1570 | | | | | 84.87 | 12.37 | 2.21 | 0.55 |
| | Manasi gas field | 61 | MN001 | $E_{1-2}z$ | 2516–2522 | 50.3 | 1.9 | 6778 | | 93.04 | 2.99 | 1.85 | 2.11 |
| | | 62 | MN1 | $E_{1-2}z$ | 2446.5–2414 | 53.3 | | | | | | | |
| | Huoerguosi | 63 | H8a | $E_{1-2}z$ | 1821.5–1826 | | | | | | | | |
| | Duzishan | 64 | D2 | $N_1s$ | 1686–1689 | 45.8 | 2.4 | | | 74.47 | 17.93 | 6.9 | 0.69 |
| | Xihu | 65 | XH1 | $J_3$ | 6139–6160 | 42.5 | 1.59 | 2074 | | 78.46 | 14.79 | 5.46 | 1.29 |
| | Kayindike | 66 | K11 | $J_3q$ | 4251–4256 | 40.7 | 2.06 | | | 82.7 | 13.98 | 2.91 | 0.41 |

[a] GOR = Gas to oil ratio.

responses of different series of diamondoids (A, MA, DMA, TMA, EA, D, MD) were obtained by the external standard method of Liang et al. (2012). First, series of isooctane solutions with different concentrations of ten diamondoid standards (A, 1-MA, 1,3-DMA, 1,3,5-TMA, 2-MA, 1-EA, 1-E-3-MA, 2-EA, D, and 1-MD) were prepared and spiked with the IS solution. Then, the solutions were introduced to the GC–MS-MS for analysis. The calibration curves were calculated using ratios of the peak area for each standard diamondoid to that of the corresponding IS ($A_{Cn}/A_{IS}$) vs the corresponding concentration ratios ($C_{Cn}/C_{IS}$). Finally, the response factors for different series of diamondoids relative to the IS were obtained according to the corresponding calibration curves.

## 3. Results and discussion

### 3.1. Concentration of diamondoids in the Junggar oils

Fig. 2a shows that oils from the four regions of the Junggar Basin have a significant variation in diamondoid concentrations: 0–7000 ppm for total adamantanes and 0–450 ppm for total diamantanes. This indicates obvious differences in hydrocarbon source or thermal maturity. In general, high diamondoid concentrations reflect high maturity, and thus oil maturity (which indicates the maturity of the source rock at the time that the source rock generated and expelled the oil) can be broadly determined from diamondoid concentrations. However, the organic matter types of the source rocks for the studied oil samples are not the same, which may also affect the diamondoid concentrations of oils at the same maturity (Wei et al., 2006b). Experiments have shown that the organic matter type has less influence on diamondoid yields than maturity at the low-mature to mature stages (Jiang et al., 2018). As such, the effect of source rock type on diamondoid concentration is not considered further in this study.

The oils can be divided into three main areas based on the concentrations of adamantanes and diamantanes as shown in Fig. 2a. Data for oils plotting in area A have a relatively low concentration of diamondoids (<100 ppm adamantanes and <5 ppm diamantanes), indicating that the crude oils in this area are at the low-mature stage. This is supported by the low API gravity of the oils in area A (Fig. 2b), given that API gravity increases with increasing oil maturity (Peters et al., 2005). Moreover, for the oils in area A, no obvious variation between diamondoid concentration and oil API gravity is observed (Fig. 2b), indicating that diamondoid evolution has not entered the thermal formation stage (the stage where diamondoids are mainly formed by the thermal degradation of the kerogen or bitumen), and that the diamondoids formed mainly during diagenesis. Therefore, for oils in area A, diamondoid concentration ratios and isomerization ratios could be used as source indicators. The distribution of biomarkers also indicates that oils in area A are at the low-mature stage. Values of $C_{29}$ ααα20S/(20S + 20R) and $C_{29}$ αββ/(ααα + αββ) of steranes in oils from area A are ~0.45 and ~0.56 (Table 2), respectively, corresponding to the early stage of the oil window (Peters et al., 2005).

The oils in area B contain 100–1000 ppm adamantanes and 5–50 ppm diamantanes, and the total diamondoid concentration displays a positive relationship with the oil API gravity (Fig. 2b). This suggests that these oils have entered the mature stage, in which

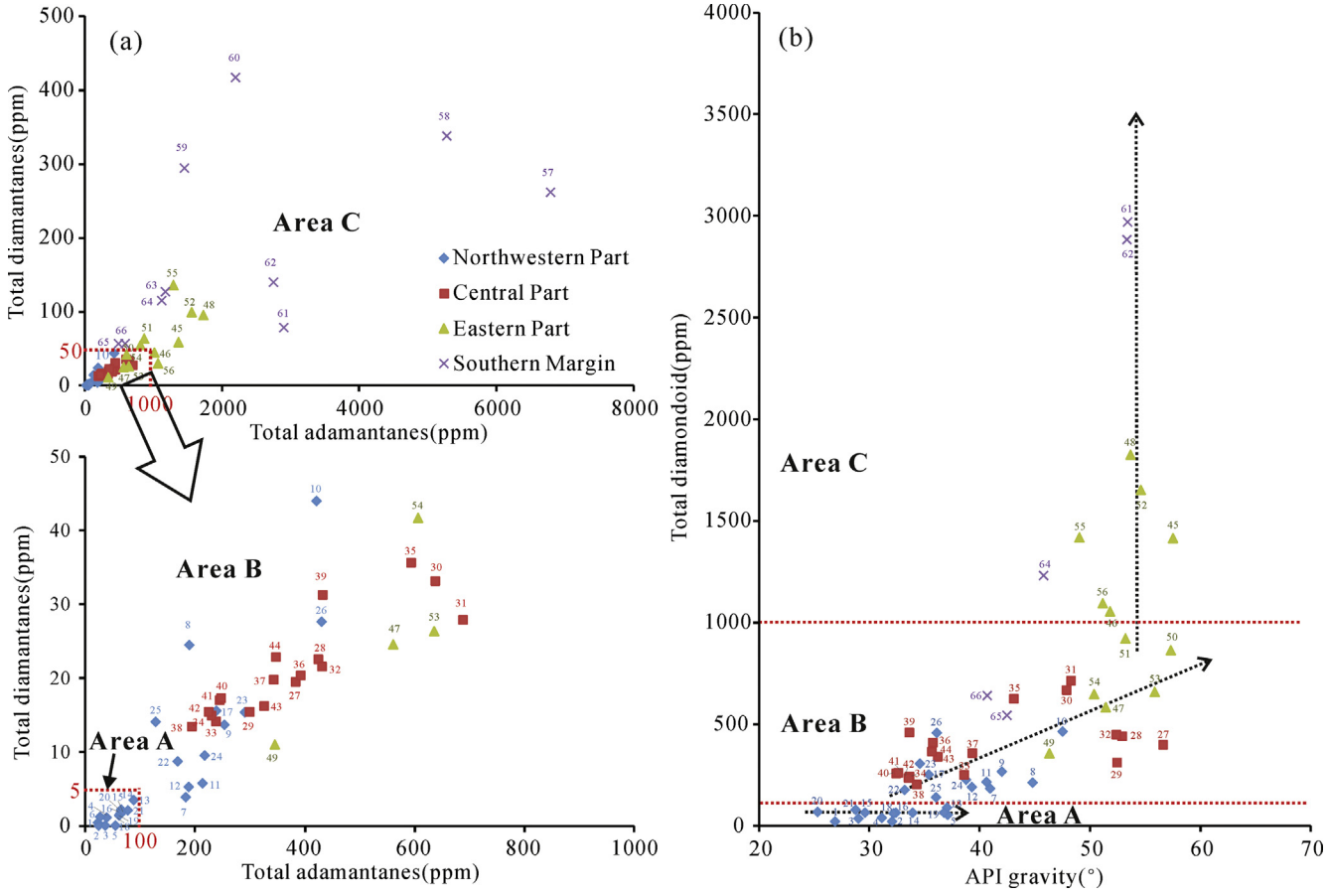


**Fig. 2.** The concentration of adamantanes vs diamantanes (a) and total diamondoids vs API gravity (b) for crude oils from the Junggar Basin.

**Table 2**
Geochemical parameters for the crude oil samples from the Junggar Basin.

| Sample number | Well | Area | As (ppm) | Ds (ppm) | Diamondoids (ppm) | $C_{29}$ ααα20S/(20S + 20R) | $C_{29}$ αββ/(ααα + αββ) | Ts/(Ts + Tm) | T/P | MPI-1 | Rc (%) |
|---|---|---|---|---|---|---|---|---|---|---|---|
| 1 | FN4 | A | 21.96 | 0.40 | 22.36 | 0.46 | 0.58 | 0.07 | 1.50 | 0.97 | 1.72 |
| 2 | FN7 | A | 23.86 | 0.00 | 23.86 | 0.48 | 0.56 | 0.11 | 1.81 | 0.94 | 1.74 |
| 3 | W35 | A | 35.53 | 0.00 | 35.53 | 0.45 | 0.47 | 0.08 | 1.32 | 0.80 | 1.82 |
| 4 | X71 | A | 38.00 | 1.05 | 39.05 | 0.46 | 0.59 | 0.57 | 0.97 | 0.65 | 1.91 |
| 5 | X72 | A | 54.66 | 0.00 | 54.66 | 0.48 | 0.61 | 0.21 | 6.25 | – | – |
| 6 | X87 | A | 26.12 | 1.20 | 27.32 | 0.46 | 0.55 | 0.34 | 0.54 | 0.73 | 1.86 |
| 7 | X94 | B | 181.54 | 3.86 | 185.40 | 0.46 | 0.59 | 0.18 | 3.56 | 0.64 | 1.91 |
| 8 | MA13 | B | 188.98 | 24.47 | 213.45 | 0.46 | 0.55 | 0.27 | 2.11 | 0.66 | 1.90 |
| 9 | MA134 | B | 252.09 | 13.65 | 265.73 | 0.47 | 0.61 | 0.14 | 4.19 | 0.79 | 1.83 |
| 10 | MA15 | B | 419.81 | 43.98 | 463.79 | 0.46 | 0.54 | 0.11 | 3.35 | 0.75 | 1.85 |
| 11 | MA18 | B | 212.66 | 5.76 | 218.42 | 0.47 | 0.71 | 0.28 | 4.88 | 0.36 | 2.08 |
| 12 | MX1 | B | 187.28 | 5.22 | 192.50 | 0.48 | 0.67 | 0.20 | 4.98 | 0.38 | 2.07 |
| 13 | AH2 | A | 87.62 | 3.41 | 91.04 | 0.47 | 0.63 | 0.35 | 3.31 | 0.42 | 2.05 |
| 14 | MH1 | A | 64.49 | 2.16 | 66.65 | 0.47 | 0.60 | 0.13 | 3.04 | – | – |
| 15 | B007 | A | 64.78 | 2.11 | 66.89 | 0.46 | 0.55 | 0.11 | 2.07 | 0.26 | 2.14 |
| 16 | B7 | A | 62.82 | 1.60 | 64.41 | 0.47 | 0.52 | 0.12 | 2.03 | 0.16 | 2.20 |
| 17 | K901 | B | 238.44 | 15.50 | 253.94 | 0.46 | 0.60 | 0.22 | 0.99 | 0.76 | 1.85 |
| 18 | K92 | A | 60.95 | 1.39 | 62.34 | 0.48 | 0.57 | 0.11 | 2.31 | 0.97 | 1.72 |
| 19 | K94 | A | 63.54 | 1.63 | 65.17 | 0.47 | 0.57 | 0.10 | 2.72 | 1.00 | 1.70 |
| 20 | HW5 | A | 67.74 | 1.84 | 69.58 | 0.47 | 0.59 | 0.11 | 2.47 | 0.58 | 1.95 |
| 21 | HW8 | A | 77.33 | 2.06 | 79.39 | 0.46 | 0.56 | 0.11 | 2.20 | 0.88 | 1.77 |
| 22 | HS4 | B | 167.35 | 8.69 | 176.04 | 0.45 | 0.54 | 0.31 | 1.96 | 1.00 | 1.70 |
| 23 | HS6 | B | 290.35 | 15.34 | 305.69 | 0.45 | 0.55 | 0.22 | 2.75 | 0.77 | 1.84 |
| 24 | G26 | B | 217.28 | 9.48 | 226.76 | 0.45 | 0.49 | 0.14 | 1.61 | 0.93 | 1.74 |
| 25 | K79 | B | 126.83 | 14.03 | 140.86 | 0.48 | 0.55 | 0.22 | 2.60 | 0.97 | 1.72 |
| 26 | ZJ2-H | B | 429.46 | 27.65 | 457.12 | 0.49 | 0.64 | 0.53 | 14.09 | 0.94 | 1.74 |
| 27 | P5 | B | 381.5 | 19.5 | 401.0 | 0.48 | 0.61 | 0.25 | 2.86 | 0.76 | 1.84 |
| 28 | M171 | B | 422.5 | 22.6 | 445.1 | 0.46 | 0.61 | 0.27 | 1.67 | 0.76 | 1.84 |
| 29 | M7 | B | 297.3 | 15.4 | 312.7 | 0.47 | 0.61 | 0.27 | 2.12 | 0.74 | 1.86 |
| 30 | M11 | B | 636.1 | 33.2 | 669.3 | 0.48 | 0.60 | 0.22 | 1.67 | 0.71 | 1.87 |
| 31 | M001 | B | 687.3 | 27.9 | 715.2 | 0.50 | 0.62 | 0.25 | 4.57 | 0.69 | 1.88 |
| 32 | QS1 | B | 430.1 | 21.6 | 451.7 | 0.47 | 0.62 | 0.27 | 3.07 | 0.77 | 1.84 |
| 33 | MB11 | B | 237.1 | 14.2 | 251.3 | 0.44 | 0.58 | 0.20 | 0.79 | 0.76 | 1.85 |
| 34 | SX8 | B | 229.2 | 14.9 | 244.1 | 0.47 | 0.58 | 0.23 | 1.17 | 0.75 | 1.85 |
| 35 | SX3 | B | 591.8 | 35.7 | 627.5 | 0.46 | 0.59 | 0.21 | 1.20 | 0.69 | 1.88 |
| 36 | SN42 | B | 390.5 | 20.3 | 410.9 | 0.48 | 0.59 | 0.41 | 1.28 | 0.65 | 1.91 |
| 37 | S303 | B | 342.4 | 19.8 | 362.1 | 0.47 | 0.59 | 0.31 | 1.46 | 0.71 | 1.87 |
| 38 | S102 | B | 192.6 | 13.5 | 206.1 | 0.46 | 0.57 | 0.27 | 1.02 | 0.54 | 1.98 |
| 39 | S123 | B | 430.6 | 31.3 | 461.9 | 0.45 | 0.59 | 0.39 | 1.31 | 0.61 | 1.94 |
| 40 | XY19 | B | 242.9 | 17.0 | 259.9 | 0.47 | 0.58 | 0.27 | 1.13 | 0.83 | 1.80 |
| 41 | XY22 | B | 245.8 | 17.4 | 263.1 | 0.47 | 0.59 | 0.27 | 1.11 | 0.84 | 1.80 |
| 42 | SN62 | B | 222.6 | 15.5 | 238.1 | 0.48 | 0.59 | 0.27 | 1.10 | 0.85 | 1.79 |
| 43 | L11 | B | 325.0 | 16.2 | 341.2 | 0.46 | 0.60 | 0.48 | 1.57 | 0.54 | 1.97 |
| 44 | L27 | B | 346.2 | 22.8 | 369.0 | 0.45 | 0.60 | 0.49 | 1.40 | 0.56 | 1.96 |
| 45 | C25 | C | 1357.7 | 58.3 | 1416.0 | – | – | – | – | – | – |
| 46 | C27 | C | 1011.8 | 45.0 | 1056.8 | – | – | – | – | – | – |
| 47 | C54 | B | 560.8 | 24.5 | 585.3 | 0.40 | 0.61 | 0.63 | 0.53 | 0.64 | 1.92 |
| 48 | C55 | C | 1728.7 | 95.5 | 1824.2 | 0.38 | 0.60 | 0.74 | 2.41 | 0.59 | 1.94 |
| 49 | DX21 | B | 344.2 | 11.0 | 355.2 | 0.41 | 0.53 | 0.65 | 0.28 | 0.50 | 2.00 |
| 50 | DX33 | C | 808.6 | 54.7 | 863.3 | – | – | – | – | – | – |
| 51 | D103 | C | 857.8 | 63.9 | 921.7 | 0.34 | 0.57 | 0.54 | 1.90 | – | – |
| 52 | DX18 | C | 1554.0 | 98.8 | 1652.8 | 0.41 | 0.61 | 0.79 | 3.05 | 0.70 | 1.88 |
| 53 | DX27 | B | 634.5 | 26.3 | 660.8 | 0.41 | 0.54 | 0.33 | 1.17 | 0.42 | 2.05 |
| 54 | DX14 | B | 606.1 | 41.7 | 647.8 | 0.41 | 0.58 | 0.74 | 2.10 | 0.64 | 1.92 |
| 55 | D403 | C | 1284.3 | 136.1 | 1420.4 | 0.35 | 0.58 | 0.80 | 1.98 | 0.62 | 1.93 |
| 56 | DX17 | C | 1066.0 | 29.8 | 1095.8 | 0.39 | 0.55 | 0.84 | 1.71 | 0.37 | 2.08 |
| 57 | H2 | C | 6785.9 | 261.4 | 7047.3 | 0.48 | 0.63 | 0.14 | 1.83 | – | – |
| 58 | H2004 | C | 5273.5 | 337.6 | 5611.1 | 0.46 | 0.56 | 0.65 | 6.92 | 0.04 | 2.27 |
| 59 | TG1 | C | 1445.3 | 294.8 | 1740.1 | 0.48 | 0.71 | 0.84 | 1.97 | – | – |
| 60 | TG2 | C | 2189.0 | 417.5 | 2606.4 | 0.48 | 0.61 | 0.81 | 1.13 | 0.81 | 1.82 |
| 61 | MN001 | C | 2892.2 | 78.3 | 2970.5 | 0.41 | 0.60 | 0.58 | 3.45 | 0.67 | 1.90 |
| 62 | MN1 | C | 2744.1 | 139.3 | 2883.5 | 0.54 | 0.66 | 0.61 | 9.23 | – | – |
| 63 | H8a | C | 1172.2 | 127.4 | 1299.6 | 0.40 | – | 0.45 | – | – | – |
| 64 | D2 | C | 1118.1 | 115.0 | 1233.1 | 0.33 | 0.43 | 0.38 | 0.16 | 0.87 | 1.78 |
| 65 | XH1 | C | 488.4 | 56.6 | 545.0 | 0.43 | 0.53 | 0.38 | 0.29 | 0.76 | 1.84 |
| 66 | K11 | C | 584.7 | 56.7 | 641.4 | 0.48 | 0.59 | 0.32 | 0.13 | – | – |

Tm: 17α(H)-22,29,30-trisnorhopane; Ts: 18α(H)-22,29,30-trisnorneohopane; T/P: tricyclic/pentacyclic terpane; G/$C_{30}$H: gammacerane/$C_{30}$ hopane; MPI-1: 1.5 (3- + 2-methylphenanthrenes)/(phenanthrene + 1- +9-methylphenanthrenes); calculated vitrinite reflectance Rc (%): $-0.6 \times$ MPI-1 + 2.30 (Radke and Welte, 1983); symbol "–": not detected.

thermogenic diamondoids have begun to be generated by thermal cracking of kerogen and bitumen, and the diamondoid concentrations increase with thermal maturity. As a result, diamondoid concentrations and concentration ratios are good indicators of thermal maturity. Compared with oils in area A, values of $C_{29}$ αββ/(ααα + αββ) for oils in area B are generally higher (~0.60, corresponding

to 0.8–0.9 %Ro; Peters et al., 2005), indicating that oils in this area are mature.

Diamondoids are enriched in oils from area C, with >1000 ppm adamantanes and >50 ppm diamantanes, indicating that these crude oils have entered the highly mature stage. In this stage, the oils are dominated by condensates with API gravity values of >50° (Fig. 2b). Conventional biomarker indices are generally not useful for the maturity assessment of these oils due to the lack of biomarkers or because the various indices have reached equilibrium. For example, $C_{29}$ αββ/(ααα + αββ) values are the same as for the oils in area B despite their different maturity level. However, given that diamondoids are more thermally stable than other hydrocarbon fractions, increasing thermal maturity leads to further diamondoid enrichment (Dahl et al., 1999). In this stage, the thermodynamic stability of diamondoid compounds becomes a critical factor in the composition and distribution of diamondoids in oil. Therefore, in some cases, diamondoid isomerization ratios may be good maturity indices for highly mature condensates.

We have shown that the thermal maturity of oils from the Junggar Basin can be assessed based on their diamondoid concentrations. Data for oils from the northwestern Junggar Basin all plot in areas A and B in Fig. 2a. These oils have relatively low concentrations of diamondoids, which mainly range from 0 to 300 ppm adamantanes and 0 to 20 ppm diamantanes, indicating that they are in the low-mature to mature stages. This is consistent with the fact that crude oils in the northwestern basin are considered to be derived from Permian source rocks and formed during the early to mature oil generation stages (Cao et al., 2005, 2006a; Wu, 2009). All oils from the central Junggar Basin plot in area B in Fig. 2a, with adamantane and diamantane concentrations of 200–700 ppm and 10–40 ppm, respectively, suggesting that oils in the central basin are in the mature stage of oil generation. This result is consistent with previous studies showing that oils in the central basin are the produced from mature Permian source rocks (Pan et al., 1999; Zou et al., 2005; Chen et al., 2010; Wang et al., 2010).

Crude oils from the Kelameili area in the eastern Junggar Basin are condensates associated with natural gases, which almost always plot in areas C and B, with concentrations of adamantanes and diamantanes ranging from 340–1800 ppm and 10–140 ppm, respectively, suggesting these oils have reached the mid-oil to early-gas window of generation. This is supported by the measured vitrinite reflectance values of the Carboniferous source rocks of these oils, which range from 0.66 %Ro to 1.80 %Ro (Da et al., 2010; Yang et al., 2012). Oils from the southern margin of the basin almost all plot in area C, demonstrating their high maturity. This result is consistent with the study of Chen et al. (2015b), which proposed that the maturity of oils in the middle section of the southern margin reached 1.4 %Ro(eq) and that the oil maturity in the western section of the southern margin was relatively lower, based on aromatic hydrocarbon indices.

### 3.2. Application of diamondoid indices for oil–oil correlations at low-mature to mature stages

Schulz et al. (2001) suggested that some diamondoid isomerization ratios, such as MAI, EAI [=1-EA/(1-EA + 2-EA)], MDI, DMDI-1 [=4,9-DMD/(4,9-DMD + 3,4-DMD)], and DMDI-2 [=4,9-DMD/(4,9-DMD + 4,8-DMD)], exhibited no systematic variations with thermal maturity in the oil window, but were related to source rock type. Our previous studies based on laboratory experiments also demonstrated that diamondoid isomerization ratios, such as DMAI-1[=1,3-DMA/(1,3-DMA + 1,2-DMA)], DMAI-2 [=1,3-DMA/(1,3-DMA + 1,4-DMA)], TMAI-1 [=1,3,5-TMA/

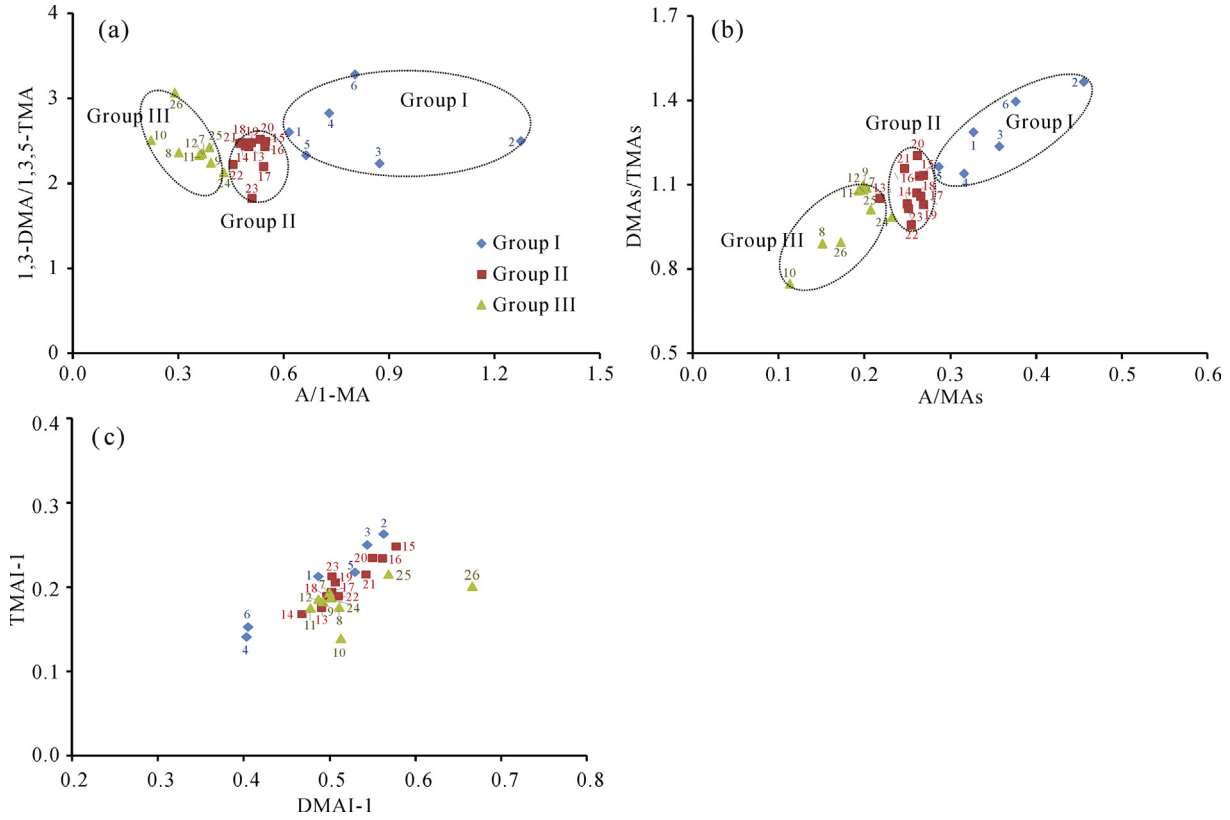


**Fig. 3.** Cross plots of diamondoid concentration ratios used for oil–oil correlation. (a) A/1-MA vs 1,3-DMA/1,3,5-TMA, (b) A/MAs vs DMAs/TMAs and (c) DMAI-1 vs TMAI-1. See Appendix A for compound name abbreviations.

(1,3,5-TMA + 1,3,4-TMA)], TMAI-2 [=1,3,5-TMA/(1,3,5-TMA + 1,3,6-TMA)], MDI, and DMDI-1, are fairly constant in the low-mature to mature stages, and that diamondoid concentration ratios (e.g., A/D, MAs/MDs, DMAs/DMDs, DMAs/MDs, and As/Ds) show no obvious changes in the low-mature stage (Fang et al., 2012, 2013; Li et al., 2015). This indicates that some diamondoid parameters might be source-dependent rather than maturity-dependent within certain maturity stages. Therefore, diamondoid indices might be useful for oil–oil correlations in relatively low maturity oils. Oils from the northwestern Junggar Basin are in the low-mature to mature stages, and thus we now explore using diamondoid indices for oil–oil correlations and compare these with previous biomarker studies.

Common diamondoid concentration ratios (e.g., A/D, MAs/MDs, DMAs/DMDs, DMAs/MDs, and As/Ds) could not be obtained in this study, as some diamantanes were present in concentrations that were below our detection limits. However, according to the experiments of Fang et al. (2013), the relative percentages of alkylated adamantanes in the oil window (0.8%–1.5% EasyRo) are nearly constant, suggesting that ratios of alkyl adamantanes do not change with maturity in this thermal stage. Thus, we attempted to use some diamondoid pairs based on adamantane concentration ratios (e.g., A/1-MA vs 1,3-DMA/1,3,5-TMA and A/MAs vs DMAs/TMAs) to differentiate the sources of the northwestern oils (Fig. 3a and b).

Oils from the northwestern basin can be divided into three groups (Table 1; Fig. 3a and b). Group I oils are located mainly in the Wuxia zone, which have relatively high diamondoid concentration ratios (e.g., A/1-MA, A/MAs, and DMAs/TMAs values of >0.6, >0.3, and >1.1, respectively; Fig. 3a and b). Group II oils are from the southwestern slope of the Mahu Depression, Kebai zone, and parts of the Zhongguai zone. Group III oils are from the northern Mahu Depression and parts of the Zhongguai zone, and have lower diamondoid concentration ratios (e.g., A/1-MA, A/MAs, and DMAs/TMAs values of <0.43, <0.23, and <1.1, respectively; Fig. 3a and b).

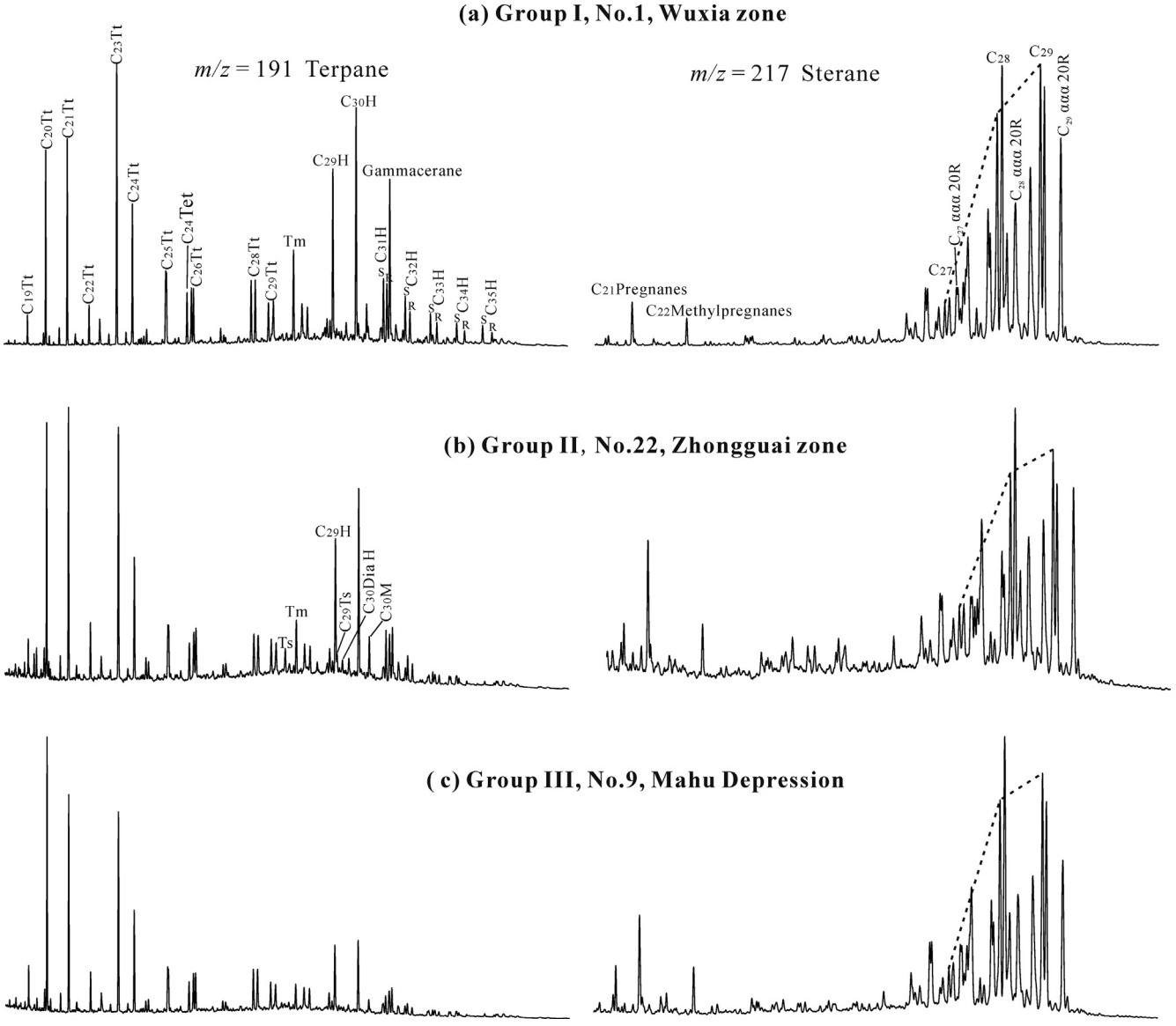


**Fig. 4.** Chromatograms for *m/z* 191 and *m/z* 217 showing terpane and sterane distributions, respectively, for typical oils from the northwestern Junggar Basin. $C_{19}$–$C_{29}$ Tt: $C_{19}$–$C_{29}$ tricyclic terpanes; $C_{24}$ Tet: $C_{24}$ tetracyclic terpane; Tm: 17α(H)-22,29,30-trisnorhopane; Ts: 18α(H)-22,29,30-trisnorneohopane; $C_{29}$ H: $C_{29}$ 17α(H),21β(H)-30-norhopane; $C_{29}$Ts: $C_{29}$ 18α(H)-30-norneohopane; $C_{30}$ DiaH: $C_{30}$ 17α(H)-diahopane; $C_{30}$ H: $C_{30}$ 17α(H),21β(H)-hopane; $C_{30}$ M: $C_{30}$ 17β(H),21α(H)-moretane; $C_{31}$–$C_{35}$ H: $C_{31}$–$C_{35}$ 17α(H),21β(H)-homohopanes.

The division is consistent with the biomarker data. As shown in Fig. 4: (a) The relative concentrations of tricyclic terpanes and gammacerane in Group I oils are higher than that in the other two groups, whereas the relative concentrations of Ts, $C_{29}$Ts, and $C_{30}$ diahopane are distinctly lower, which is the characteristic of oils from the $P_{1f}$ formation (Chen et al., 2016a, 2016b; Huang, 2017). (b) Tricyclic terpanes and gammacerane in Group II oils occur at lower concentrations than in the Group I oils, while the Ts content is obviously higher than that in the Group I oils, which is consistent with oils sourced from the $P_{2w}$ formation (Chen et al., 2016a, 2016b; Huang, 2017). (c) Group III oils have a high abundance of tricyclic terpanes, but an obviously lower content of hopanes, indicating another source for these oils. According to the higher diamondoid concentrations of the Group III oils than those of Group I and II oils (Table 2), we propose that Group III oils were derived from a relatively mature source rock ($P_{1j}$ or $P_{1f}$) in the deep Mahu Depression. The groupings found in the present study are also consistent with previous work based on biomarker distributions (Chen et al., 2016a, 2016b).

Unlike the diamondoid concentration ratios, the diamondoid isomerization ratios of all of these oils are similar. For example, DMAI-1 and TMAI-1 values of the three oil groups are 0.4–0.6 and 0.1–0.3, respectively (Fig. 3c), indicating that although the diamondoid isomerization ratios are independent of maturity in the low-mature to mature stages, they are also not useful for source tracing in the case of these Junggar oils.

### 3.3. Application of diamondoid indices to determine oil thermal maturity

As noted earlier, crude oils in the Junggar Basin can be broadly classified into three maturity stages: low-mature, mature (normal oil), and highly mature (condensate oil) based on diamondoid concentrations and so it is preferable to have more parameters to

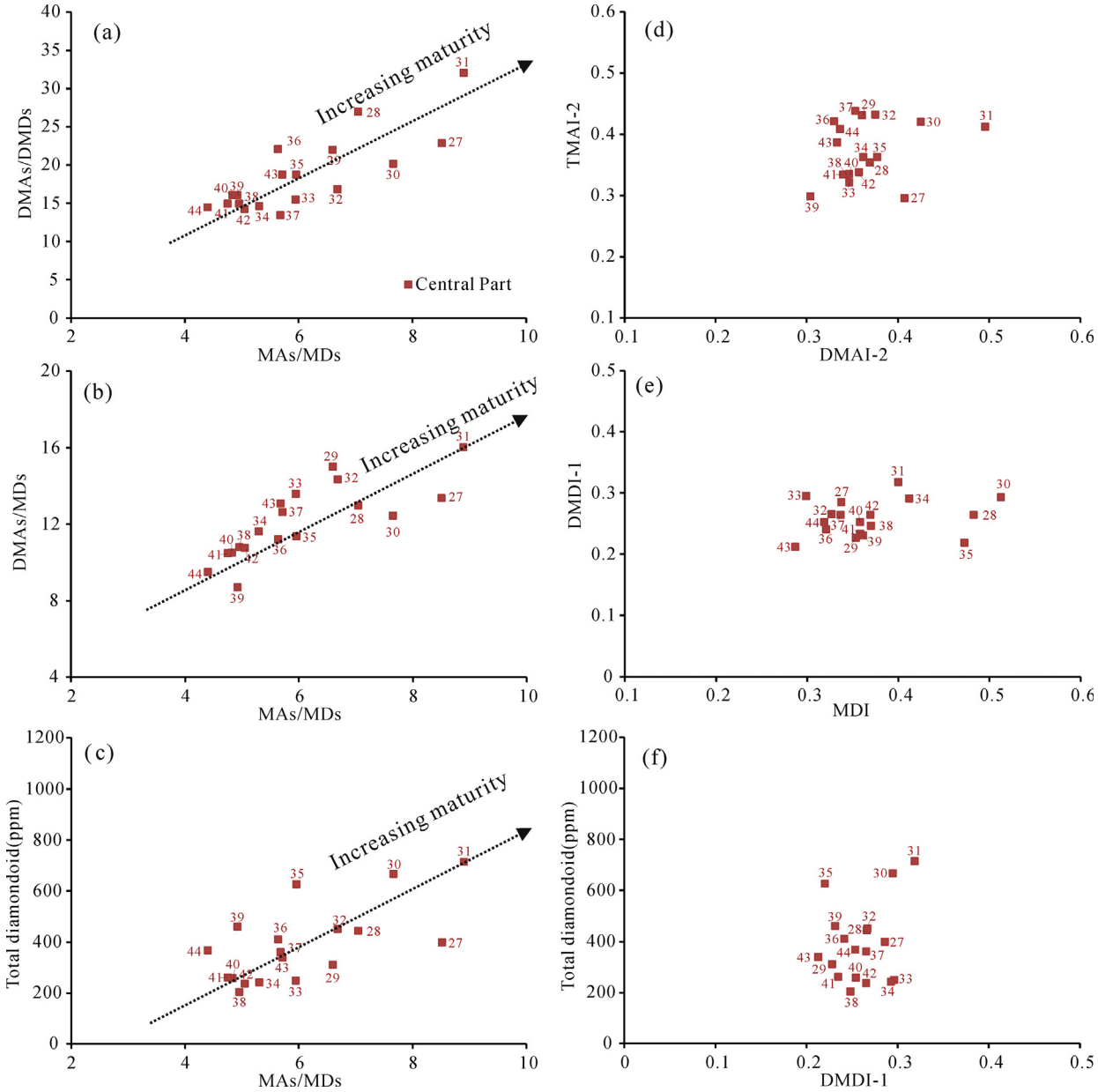


**Fig. 5.** Specific diamondoid concentration ratios reflecting maturity of oils from the central Junggar Basin. (a) MAs/MDs vs DMAs/DMDs, (b) MAs/MDs vs DMAs/MDs, (c) MAs/MDs vs total diamondoids, (d) DMAI-2 vs TMAI-2, (e) MDI vs DMDI-1, and (f) DMDI-1 vs total diamondoids. See Appendix A for abbreviations of compound names.

accurately ascertain oil maturity. For low-mature oils, conventional biomarker ratios, such as 20S/(20S + 20R) and αββ/(αββ + ααα) for the $C_{29}$ steranes, 22S/(22S + 22R) for $C_{31}$ hopanes, and Ts/(Ts + Tm), are effective and readily acquired. However, for some mature oils and condensates, most biomarker maturity indicators are not useful or cannot be obtained. Our previous pyrolysis experimental studies (Fang et al., 2012, 2013; Li et al., 2015; Jiang et al., 2018) have demonstrated that diamondoid indices are potential maturity indicators for mature and highly mature oils and/or source rocks. Recently, diamondoid indices have been used successfully for the maturity assessment of Tarim Basin oils (Li et al., 2018). Thus, in the following section we consider how diamondoid indices can be used to assess the thermal maturity of the different crude oil types in the Junggar Basin.

### 3.3.1. Mature oils

The crude oils from the central Junggar Basin are mainly mature oils, which plot in area B in Fig. 2a. Table 2 shows that the $C_{29}$ 20S/(20S + 20R) and $C_{29}$ αββ/(αββ + ααα) sterane ratios for most of these oils are around 0.48 and 0.60, respectively, and hence conventional sterane and hopane biomarker maturity indicators are close to equilibrated and therefore not very useful.

We have found that from 1.0% to 1.5% EasyRo (i.e., the oil generation stage) some diamondoid concentration ratios (MAs/MDs, DMAs/MDs, DMAs/DMDs, and As/Ds) can rapidly increase with maturity, whereas diamondoid isomerization ratios exhibit little variation in this stage (Fang et al., 2013, 2015; Jiang et al., 2018). As such, diamondoid concentration ratios (MAs/MDs, DMAs/MDs, DMAs/DMDs, and As/Ds) are useful for assessing the thermal maturities of source rocks or oils in the oil window.

For our samples, there appears to be a positive linear correlation in our oils between MAs/MDs and DMAs/DMDs ratios (Fig. 5a). Higher diamondoid concentration ratios reflect higher oil maturities. Based on the indices shown in Fig. 5a, we conclude that the thermal maturity of these oils displays a generally increasing trend from north to south in the central Junggar Basin (the sample number of these oils decreases from north to south). This might be the result of oil migration, given that oil migrated from north to south along the south-dipping slope in the central basin, thus causing the change of maturities of the oils (Cai and Liu, 2005). A plot of MAs/MDs vs DMAs/MDs (Fig. 5b) shows a similar trend to that in Fig. 5a. The potential of maturity assessment by diamondoid concentration ratios is also highlighted by Fig. 5c, in which the total diamondoid concentration positively correlates with MAs/MDs. Therefore, some diamondoid concentration ratios (e.g., MAs/MDs, DMAs/MDs, and DMAs/DMDs) can be used to determine oil maturity in the oil window, at least for the Junggar Basin.

Diamondoid isomerization ratios of oils in the central basin exhibit little variability (Fig. 5d and e), with DMAI-2, TMAI-2, and MDI values that are mainly in the range 0.3–0.5 and DMDI-1 values of 0.2–0.3. Fig. 5f also shows that DMDI-1 does not obviously change with total diamondoid concentrations, suggesting that isomerization ratios are ineffective for maturity assessment in the oil window, which is consistent with laboratory experiments (Fang et al., 2012, 2013; Li et al., 2015).

### 3.3.2. Condensates

Most of the samples from the eastern and southern margins of the Junggar Basin are condensates with high maturities (Fig. 2a). In this stage, most conventional biomarker maturity indicators are

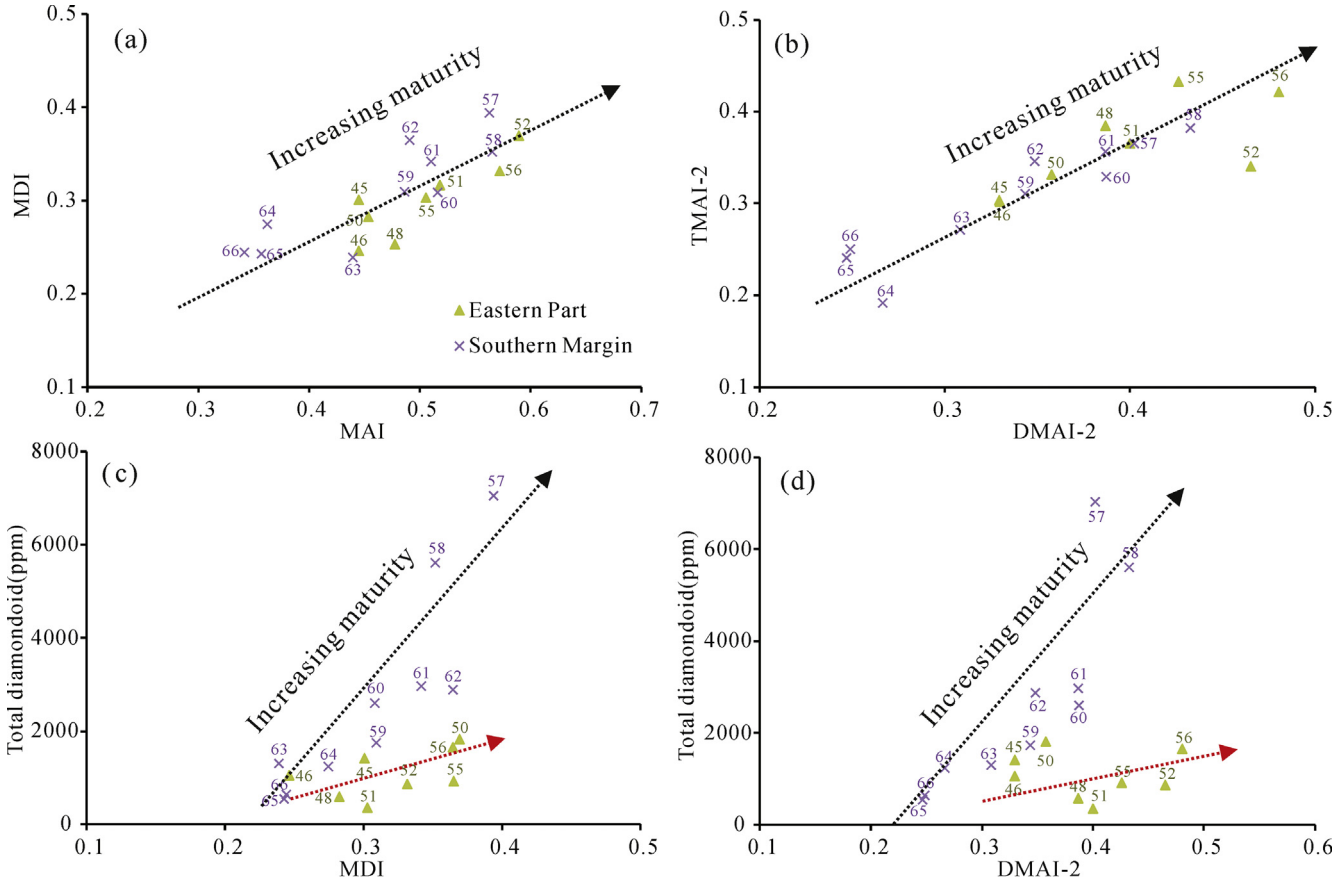


**Fig. 6.** Diamondoid isomerization ratios reflecting maturity of condensates from Kelameili zone (Eastern Part) and South Margin in the Junggar Basin. (a) MAI vs MDI, (b) DMAI-2 vs TMAI-2, (c) MDI vs total diamondoids, and (d) DMAI-2 vs total diamondoids. See Appendix A for abbreviations of compound names.

invalid, and only a few indices may be effective, such as MPI-1, which exhibits a good negative linear correlation with %Ro in the highly mature range (1.35–2.00 %Ro; Radke and Welte, 1983). The equivalent vitrinite reflectance (Rc; calculated from its relationship with MPI-1) of oils in the eastern and southern margin of the Junggar Basin ranges from 1.88% to 2.27% (Table 2), indicating that these oils have entered the high- to over-mature stages. However, in some cases, aromatic maturity indices cannot be determined accurately due to the low concentrations of aromatic hydrocarbons in condensate oils. For example, in some oils in the eastern and southern margin of the Junggar Basin, methylphenanthrenes (MPI-1) are not measurable because of low compound concentrations (Table 2). Diamondoid isomerization ratios have proven to be useful maturity indicators at a maturity of over 1.5% EasyRo (i.e., the oil cracking stage; Chen et al., 1996; Li et al., 2000, 2015; Zhang et al., 2005; Wei et al., 2007b; Fang et al., 2012, 2013; Jiang et al., 2018). Thus, in this range it might be possible to assess the maturity of condensates using diamondoid isomerization ratios.

There is a good positive correlation between different diamondoid isomerization ratios for the oil samples from the Kelameili zone in the eastern part of the basin and along its southern margin (both plot in area C in Fig. 2a). These include plots of MAI vs MDI and DMAI-2 vs TMAI-2 (Fig. 6a and b). According to our experiments (Fang et al., 2013; Jiang et al., 2018), diamondoid isomerization ratios are useful at higher thermal maturities. Hence, it could be inferred that the maturity of source rocks for the oils in the Kelameili zone increases from east to west. This is consistent with source rock data, which show that the source rocks in the western Kelameili zone have %Ro > 1.5, decreasing to the east (Xu, 2005; Da et al., 2010; Long et al., 2014; Xiang et al., 2016). Similarly, oils from the middle section of the southern margin are more mature than those from the western section (the number of samples increases from middle to west). This is consistent with the study of Chen et al. (2015a, 2015b), which showed that oil maturity from the middle section of the southern margin had a %Ro(eq) of 1.4 and decreases to the west.

There is a positive relationship between the total diamondoid concentrations and diamondoid isomerization ratios (e.g., MDI and DMAI-2; Fig. 6c and d) in oils from the Kelameili zone and the southern margin, reflecting the applicability of maturity evaluation using these parameters (Fig. 2a). In general, at the same diamondoid isomerization ratio, the corresponding diamondoid concentrations of oils from the Kelameili zone are significantly lower than those of oils from the southern margin. We attribute this to different source rock types. Oils in the Kelameili zone and southern margin of the basin were generated from coal measures and lacustrine sapropel-type source rocks, respectively. Our previous work has revealed that the yield of diamondoids from types I and II organic matter is higher than that from Type III organic matter at the same maturity level, particularly in higher maturity stages (Jiang et al., 2018). However, the organic matter type of source rocks has little effect on diamondoid isomerization ratios (Jiang et al., 2018), indicating again that diamondoid isomerization ratios can be used to assess the maturity of highly mature oils independent of the organic matter type of their source.

## 4. Conclusions

Oils from the Junggar Basin can be broadly divided into three maturity stages according to diamondoid concentrations, which are low-mature (0–100 ppm adamantanes; 0–5 ppm diamantanes), mature (100–1000 ppm adamantanes; 5–50 ppm diamantanes), and highly mature (>1000 ppm adamantanes; >50 ppm diamantanes). Thermal maturity of the source rock for these oils increases from the northwestern basin, to the central basin, and to the eastern and southern margin of the basin.

For oils in the low-mature to mature stages, some diamondoid concentration ratios (i.e., A/1-MA, 1,3-DMA/1,3,5-TMA, A/MAs, and DMAs/TMAs) can be used for oil–oil correlations. Oils from the northwestern Junggar Basin sourced from different Permian formations can be differentiated based on these diamondoid concentration indices, as Group I, II, and III oils were derived from the $P_{1f}$, $P_{2w}$, and relatively more mature $P_{1j}$ or $P_{1f}$ source rocks in the Mahu Depression, respectively.

Different diamondoid indices are applicable at different thermal maturity ranges. Some diamondoid concentration ratios (MAs/MDs, DMAs/MDs, and DMAs/DMDs) can be used for assessing the maturity of mature oils. Based on these diamondoid concentration ratios, it can be concluded that the maturity of the source rocks for the mature oils in the central Junggar Basin decreases from south to north. Diamondoid isomerization ratios (e.g., MAI, MDI, DMAI-2, and TMAI-2) are effective for determining the maturity of condensates (i.e., oils at the high- to over-mature stages). According to diamondoid isomerization ratios, the maturity of the source rocks for the condensates from the Kelameili zone in the eastern Junggar Basin increases from east to west, and oils from the middle section of the southern margin of the basin are more mature than those in the western section.

This study shows the limitations of different diamondoid indices. Because our conclusions are based only on our field study of the Junggar Basin, more data may need to be analyzed in order to apply our conclusions to other basins.

## Acknowledgements

This work was supported by the National Natural Science Foundation of China (Grant numbers 41773034 and 41372138); and Youth Innovation Promotion Association, Chinese Academy of Sciences (Grant No. 2018386), and the Self-Research Foundation of State Key Laboratory of Organic Geochemistry, Guangzhou Institute of Geochemistry, Chinese Academy of Sciences (Grant number SKLOG2016-A02). This is Contribution number IS-2634 from GIGCAS. We are particularly grateful to Drs. Jeremy Dahl, Zhibin Wei, and Joe Curiale (Associate Editor) for their helpful comments and suggestions which substantially improved our manuscript and we really appreciate Drs. Jeremy Dahl, Joe Curiale and John Volkman for their help on improving the English expression.

## Appendix A

The abbreviations of diamondoids and definitions of diamondoid indices used in this study

| Abbreviation | Diamondoid compound | Abbreviation | Formula |
|---|---|---|---|
| A | Adamantane | MAI | 1-MA/(1-MA + 2-MA) |
| 1-MA | 1-Methyladamantane | EAI | 1-EA/(1-EA + 2-EA) |
| 1,3-DMA | 1,3-Dimethyladamantane | DMAI-1 | 1,3-DMA/(1,3-DMA + 1,2-DMA) |

**Appendix A** (*continued*)

| Abbreviation | Diamondoid compound | Abbreviation | Formula |
|---|---|---|---|
| 1,3,5-TMA | 1,3,5-Trimethyladamantane | DMAI-2 | 1,3-DMA/(1,3-DMA + 1,4-DMA) |
| 2-MA | 2-Methyladamantane | TMAI-1 | 1,3,5-TMA/(1,3,5-TMA + 1,3,4-TMA) |
| 1,4-DMA(*cis*) | 1,4-Dimethyladamantane(cis) | TMAI-2 | 1,3,5-TMA/(1,3,5-TMA + 1,3,6-TMA) |
| 1,4-DMA(*trans*) | 1,4-Dimethyladamantane(trans) | MDI | 4-MD/(4-MD + 1-MD + 3-MD) |
| 1,3,6-TMA | 1,3,6-Trimethyladamantane | DMDI-1 | 4,9-DMD/(4,9-DMD + 3,4-DMD) |
| 1,2-DMA | 1,2-Dimethyladamantane | DMDI-2 | 4,9-DMD/(4,9-DMD + 4,8-DMD) |
| 1,3,4-TMA(*cis*) | 1,3,4-Trimethyladamantane(cis) | As/Ds | Adamantanes/Diamantanes |
| 1,3,4-TMA(*trans*) | 1,3,4-Trimethyladamantane(trans) | A/D | Adamantane/Diamantane |
| 1-EA | 1-Ethyladamantane | MAs/MDs | Methyladamantanes/Methyldiamantanes |
| 2,6- + 2,4-DMA | 2,6-+2,4-Dimethyladamantane | DMAs/MDs | Dimethyladamantanes/Methyldiamantanes |
| 1,2,3-TMA | 1,2,3-Trimethyladamantane | DMAs/DMDs | Dimethyladamantanes/Dimethyldiamantanes |
| 2-EA | 2-Ethyladamantane | A/1-MA | Adamantane/1-Methyladamantane |
| D | Diamantane | 1,3-DMA/1,3,5-TMA | 1,3-Dimethyladamantane/1,3,5-Trimethyladamantane |
| 4-MD | 4-Methyldiamantane | A/MAs | Adamantane/Methyladamantanes |
| 4,9-DMD | 4,9-Dimethyldiamantane | DMAs/TMAs | Dimethyladamantanes/Trimethyladamantanes |
| 1-MD | 1-Methyldiamantane | | |
| 1,4- + 2,4-DMD | 1,4- + 2,4-Dimethyldiamantane | | |
| 4,8-DMD | 4,8-Dimethyldiamantane | | |
| 3-MD | 3-Methyldiamantane | | |
| 3,4-DMD | 3,4-Dimethyldiamantane | | |

## Appendix B. Supplementary material

Supplementary data to this article can be found online at https://doi.org/10.1016/j.orggeochem.2019.01.004.

*Associate Editor*—**Joe Curiale**

## References


Cai, X.Y., Liu, C.H., 2005. Main factors for controlling formation of oil gas reservoir in central part of Junggar Basin. Acta Petrolei Sinica 26, 1–4 (in Chinese with English abstract).

Cao, J., Zhang, Y.J., Hu, W.X., Yao, S.P., Wang, X.L., Zhang, Y.Q., Tang, Y., 2005. The Permian hybrid petroleum system in the northwest margin of the Junggar Basin, northwest China. Marine and Petroleum Geology 22, 331–349.

Cao, J., Hu, W.X., Yao, S.P., Zhang, Y.J., Wang, X.L., Zhang, Y.Q., Tang, Y., 2006a. Evolution of petroleum migration and accumulation in the northwestern margin of the Junggar Basin fluid inclusion geochemistry. Geological Review 52, 700–707 (in Chinese with English abstract).

Cao, J., Yao, S.P., Jin, Z.J., Hu, W.X., Zhang, Y.J., Wang, X.L., Zhang, Y.Q., Tang, Y., 2006b. Petroleum migration and mixing in the northwestern Junggar Basin (NW China): constraints from oil-bearing fluid inclusion analyses. Organic Geochemistry 37, 827–846.

Clayton, J.L., Yang, J., King, J.D., Lillis, P.G., Warden, A., 1997. Geochemistry of oils from the Junggar Basin, northwest China. American Association of Petroleum Geologists Bulletin 81, 1926–1944.

Chen, J.H., Fu, J.M., Sheng, G.Y., Liu, D.H., Zhang, J.J., 1996. Diamondoid hydrocarbon ratios: novel maturity indices for highly mature crude oils. Organic Geochemistry 25, 179–190.

Chen, J.P., Liang, D.G., Wang, X.L., Deng, C.P., Xue, X.K., Jin, T., Song, F.Q., Zhong, N.N., 2003a. Oil–source correlation of mixed oils derived from multiple source rocks in the Cainan Oilfield, Junggar Basin, Northwest China. Part I: fundamental geochemical features of source rocks. Petroleum Exploration and Development 30, 20–24 (in Chinese with English abstract).

Chen, J.P., Liang, D.G., Wang, X.L., Deng, C.P., Xue, X.K., Jin, T., Song, F.Q., Zhong, N.N., 2003b. Oil–source correlation of mixed oils derived from multiple source rocks in the Cainan Oilfield, Junggar Basin, Northwest China. Part II: geochemical characteristics, typing and oil sources of typical crude oils. Petroleum Exploration and Development 30, 34–38 (in Chinese with English abstract).

Chen, J.P., Deng, C.P., Liang, D.G., Wang, X.L., Shi, X.P., Jin, T., Zhong, N.N., 2004. The Cainan Oilfield: a typical mixed crude oil of three-endmember. Acta Sedimentologica Sinica 22, 91–97 (in Chinese with English abstract).

Chen, S.J., Zhan, Y., Lu, J.G., Lu, L.C., Chen, X., Wang, Y., 2010. Cretaceous hydrocarbon formation and migration direction in Well Shinan 31 in the hinterland of Junggar Basin. Petroleum Geology and Experiment 32, 382–386 (in Chinese with English abstract).

Chen, J.P., Wang, X.L., Deng, C.P., Zhao, Z., Ni, Y.Y., Sun, Y.G., Yang, H.B., Wang, H.T., Liang, D.G., Zhu, R.K., Peng, X.L., 2015a. Geochemical features of source rocks in the southern margin, Junggar Basin, Northwestern China. Acta Geologica Sinica 36, 767–780 (in Chinese with English abstract).

Chen, J.P., Wang, X.L., Deng, C.P., Zhao, Z., Ni, Y.Y., Sun, Y.G., Yang, H.B., Wang, H.T., Liang, D.G., 2015b. Geochemical features and classification of crude oils in the southern margin of Junggar Basin, Northwestern China. Acta Geologica Sinica 36, 1315–1331 (in Chinese with English abstract).

Chen, J.P., Wang, X.L., Deng, C.P., Liang, D.G., Zhang, Y.Q., Zhao, Z., Ni, Y.Y., Zhi, D.M., Yang, H.B., Wang, Y.T., 2016a. Geochemical features of source rocks and crude oil in the Junggar Basin, Northwest China. Acta Geologica Sinica 90, 37–67 (in Chinese with English abstract).

Chen, J.P., Wang, X.L., Deng, C.P., Liang, D.G., Zhang, Y.Q., Zhao, Z., Ni, Y.Y., Zhi, D.M., Yang, H.B., Wang, Y.T., 2016b. Oil and gas source, occurrence and petroleum system in the Junggar Basin, Northwest China. Acta Geologica Sinica 90, 421–450 (in Chinese with English abstract).

Chen, J.P., Wang, X.L., Deng, C.P., Zhao, Z., Ni, Y.Y., Sun, Y.G., Yang, H.B., Wang, H.T., Liang, D.G., 2016c. Investigation of typical reservoirs and occurrence regularity of crude oils in the southern margin of Junggar Basin, Northwestern China. Acta Geologica Sinica 37, 415–429 (in Chinese with English abstract).

Da, J., Hu, Y., Zhao, M.J., Song, Y., Xiang, B.L., Qin, S.F., 2010. Feature of source rock s and hydrocarbon pooling in the Kelameili gasfield, the Junggar Basin. Oil and Gas Geology 31, 187–192 (in Chinese with English abstract).

Dahl, J.E., Moldowan, J.M., Peters, K., Claypool, G., Rooney, M., Michael, G., Mello, M., Kohnen, M., 1999. Diamondoid hydrocarbons as indicators of oil cracking. Nature 399, 54–56.

Fang, C.C., Xiong, Y.Q., Liang, Q.Y., Li, Y., 2012. Variation in abundance and distribution of diamondoids during oil cracking. Organic Geochemistry 47, 1–8.

Fang, C.C., Xiong, Y.Q., Li, Y., Liu, J.Z., 2013. The origin and evolution of adamantanes and diamantanes in petroleum. Geochimica et Cosmochimica Acta 120, 109–120.

Fang, C.C., Xiong, Y.Q., Li, Y., Chen, Y., Tang, Y.J., 2015. Generation and evolution of diamondoids in source rock. Marine and Petroleum Geology 67, 197–203.

Grice, K., Alexander, R., Kagi, R.I., 2000. Diamondoid hydrocarbon ratios as indicators of biodegradation in Australian crude oils. Organic Geochemistry 31, 67–73.

He, D.F., Chen, X.F., Zhang, Y.J., Kuang, J., Shi, X., Zhang, L.P., 2004. Enrichment characteristics of oil and gas in Junggar basin. Acta Petrolei Sinica 25, 1–10 (in Chinese with English abstract).

Huang, P., 2017. The Oil-Source Correlation of Crude Oils and Source Rocks from the Northwestern Margin of Junggar Basin. University of Chinese Academy of Sciences.

Jiang, W.M., Li, Y., Xiong, Y.Q., 2018. The effect of organic matter type on formation and evolution of diamondoids. Marine and Petroleum Geology 89, 714–720.

Jin, Z.J., Cao, J., Hu, W.X., Zhang, Y., Yao, S.P., Wang, X.L., Zhang, Y.Q., Tang, Y., Shi, X., 2008. Episodic petroleum fluid migration in fault zones of the northwestern Junggar Basin (northwest China): evidence from hydrocarbon-bearing zoned calcite cement. American Association of Petroleum Geologists Bulletin 92, 1225–1243.

Kuang, L.C., Tang, Y., Lei, D.W., Wu, T., Qu, J.H., 2014. Exploration of fan-controlled large-area lithologic oil reservoirs of Triassic Baikouquan Formation in slope zone of Mahu Depression in Junggar Basin. China Petroleum Exploration 19, 14–23 (in Chinese with English abstract).

Li, J.G., Philp, P., Cui, M.Z., 2000. Methyl diamantane index (MDI) as a maturity parameter for Lower Palaeozoic carbonate rocks at high maturity and overmaturity. Organic Geochemistry 31, 267–272.

Li, P.L., 2005. Petroleum geological characteristics and exploration orientation of large oil fields in Junggar Basin. Acta Petrolei Sinica 26, 7–9 (in Chinese with English abstract).
Li, Y., Chen, Y., Xiong, Y.Q., Wang, X.T., Fang, C.C., Zhang, L., Li, J.H., 2015. Origin of adamantanes and diamantanes in marine source rock. Energy and Fuels 29, 8188–8194.
Li, Y., Xiong, Y.Q., Liang, Q.Y., Fang, C.C., Chen, Y., Wang, X.T., Liao, Z.W., Peng, P.A., 2018. The application of diamondoid indices in the Tarim oils. American Association of Petroleum Geologists Bulletin 101, 267–291.
Liang, Q.Y., Xiong, Y.Q., Fang, C.C., Li, Y., 2012. Quantitative analysis of diamondoids in crude oils using gas chromatography–triple quadruple mass spectrometry. Organic Geochemistry 43, 83–91.
Long, H.S., Li, J., Wang, X.L., Wei, L.C., Xie, Z.Y., Liao, J.D., Xiang, C.F., 2014. Effective hydrocarbon kitchen in Kelameili gas field of Junggar Basin and its control on hydrocarbon accumulation. Xinjiang Petroleum Geology 35, 500–506 (in Chinese with English abstract).
Pan, C.C., Fu, J.M., Sheng, G.Y., Yang, J.Q., 1999. The determination of oil sources and its significance in the central Junggar basin. Acta Petrolei Sinica 20, 27–32 (in Chinese with English abstract).
Pan, C.C., Yang, J.Q., Fu, J.M., Sheng, G.Y., 2003. Molecular correlation of free oil and inclusion oil of reservoir rock in the Junggar Basin, China. Organic Geochemistry 34, 357–374.
Peters, K.E., Walters, C.C., Moldowan, J.M., 2005. The Biomarker Guide. Biomarkers and Isotopes in Petroleum Systems and Earth History. Cambridge University Press, New York.
Radke, M., Welte, D.H., 1983. The methylphenanthrene index (MPI): a maturity parameter based on aromatic hydrocarbons. In: Bjorøy, M., Albrecht, P., Cornford, C., de Groot, K., Eglinton, G., Galimov, E., Leythaeuser, D., Pelet, R., Rullkötter, J., Speers, G. (Eds.), Advances in Organic Geochemistry 1981. John Wiley and Sons, New York, pp. 504–512.
Schulz, L.K., Wilhelms, A., Rein, E., Steen, A.S., 2001. Application of diamondoids to distinguish source rock facies. Organic Geochemistry 32, 365–375.
Wang, S.J., He, L.J., Wang, J.Y., 2001. Thermal regime and petroleum systems in Junggar basin, northwest China. Physics of the Earth and Planetary Interiors 126, 237–248.
Wang, X.L., Gao, G., Yang, H.B., Liu, G.D., Huang, Z., Wei, H., 2008. Research on relation between oil properties and petroleum pool formation of Permian in the 5th & 8th districts, northwestern margin of Junggar Basin. Geological Journal of China Universities 14, 256–261 (in Chinese with English abstract).
Wang, X.L., Cao, J., Shi, X.P., Xiang, B.L., Lan, W.F., Sun, P.G., 2010. A new method for studying petroleum migration and accumulation: a case study of petroleum migration and accumulation type in the Luxi area of the Junggar Basin. Earth Science Frontiers 17, 315–324 (in Chinese with English abstract).
Wang, X.L., Zhi, D.M., Wang, Y.T., Chen, J.P., Jin, Z.J., Liu, D.G., Xiang, Y., Lan, W.F., Li, N., 2013. Geochemistry of Source Rock and Petroleum in the Junggar Basin. Petroleum Industry Press, Beijing, pp. 1–565 (in Chinese with English abstract).
Wang, Y.T., 1997. Genetic classification of oils and prediction of favorable oil-bearing zones in Lunan arch in the hinterland of Junggar Basin. Xinjiang Petroleum Geology 18, 225–230 (in Chinese with English abstract).
Wei, Y.J., Zhang, Y.J., Dong, D.Z., Han, Y.K., 2006a. Current situation of natural gas exploration and its countermeasures in Junggar basin. Petroleum Exploration and Development 33, 267–273 (in Chinese with English abstract).
Wei, Z.B., Moldowan, J.M., Jarvie, D.M., Hill, R., 2006b. The fate of diamondoids in coals and sedimentary rocks. Geology 34, 1013–1016.
Wei, Z.B., Moldowan, J.M., Peters, K.E., Wang, Y., Xiang, W., 2007a. The abundance and distribution of diamondoids in biodegraded oils from the San Joaquin Valley: implications for biodegradation of diamondoids in petroleum reservoirs. Organic Geochemistry 38, 1910–1926.
Wei, Z.B., Moldowan, J.M., Zhang, S.C., Hill, R., Jarvie, D.M., Wang, H.T., Song, F.Q., Fago, F., 2007b. Diamondoid hydrocarbons as a molecular proxy for thermal maturity and oil cracking: geochemical models from hydrous pyrolysis. Organic Geochemistry 38, 227–249.
Williams, J.A., Bjorøy, M., Dolcater, D.L., Winters, J.C., 1986. Biodegradation in South Texas Eocene oils – effects on aromatics and biomarkers. Organic Geochemistry 10, 451–461.
Wingert, W.S., 1992. GC–MS analysis of diamondoid hydrocarbons in Smackover Petroleums. Fuel 71, 37–43.
Wu, K.Y., 2009. Research on the stages of reservoir formation in Wuerhe-Xiazijie Area in Junggar Basin. Journal of Oil and Gas Technology 31, 18–23 (in Chinese with English abstract).
Xiang, C.F., Wang, X.L., Wei, L.C., Li, J., Liang, T.C., Liao, J.D., 2016. Origins of the natural gas and its migration and accumulation pathways in the Kelameili Gasfield. Natural Gas Geoscience 27, 268–277 (in Chinese with English abstract).
Xu, X.Y., 2005. Study on the Carboniferous source rocks in Kelameili Area, eastern Junggar Basin. Petroleum Geology and Recovery Efficiency 12, 38–41 (in Chinese with English abstract).
Yang, B., Yan, Z.M., You, Q.M., Han, J., Guan, Q., Ren, J.L., Wu, J.Y., 2002. Geochemical characteristics of Carboniferous crude oils in Jundong area. Xinjiang Petroleum Geology 23, 478–481 (in Chinese with English abstract).
Yang, D.S., Chen, S.J., Li, L., Lu, J.G., 2012. Hydrocarbon origins and their pooling characteristics of the Kelameili Gas Field. Natural Gas Industry 32, 27–31 (in Chinese with English abstract).
Yin, W., Zheng, H.R., Meng, X.L., You, W.F., 2005. Geochemical behaviors of crude oils in central Junggar Basin. Oil and Gas Geology 26, 461–466 (in Chinese with English abstract).
Zhang, S.C., Huang, H.P., Xiao, Z.Y., Liang, D.G., 2005. Geochemistry of Palaeozoic marine petroleum from the Tarim Basin, NW China. Part 2: maturity assessment. Organic Geochemistry 36, 1215–1225.
Zheng, J.P., Sun, M., Zhao, G.C., Robinson, P.T., Wang, F.Z., 2007. Elemental and Sr–Nb–Pb isotopic geochemistry of late Paleozoic volcanic rocks beneath the Junggar basin, NW China: implications for the formation and evolution of the basin basement. Journal of Asian Earth Sciences 29, 778–794.
Zou, H.Y., Hao, F., Zhang, Q.B., Chen, B., 2005. History of hydrocarbon-filling and remigrating in hinterland of the Junggar Basin. Chinese Journal of Geology 40, 499–509 (in Chinese with English abstract).